Classifying DME vs Normal SD-OCT volumes: A review

Joan Massich*, Mojdeh Rastgoo*†, Guillaume Lemaître*†, Carol Y. Cheung*,

Tien Y. Wong†, Désiré Sidibé†, Fabrice Mériaudeau*§

*LE2I UMR6306, CNRS, Arts et Métiers, Univ. Bourgogne Franche-Comté,

12 rue de la Fonderie, 71200 Le Creusot, France

†ViCOROB, Universitat de Girona, Campus Montilivi, Edifici P4, 17071 Girona, Spain

‡Singapore Eye Research Institute, Singapore National Eye Center, Singapore

§Centre for Intelligent Signal and Imaging Research (CISIR), Electrical & Electronic Engineering Department,

Universiti Teknologi Petronas, 32610 Seri Iskandar, Perak, Malaysia

¶Corresponding author: joan.massich@u-bourgogne.fr

Abstract—This article reviews the current state of automatically classify Spectral Domain OCT (SD-OCT) data to identify Diabetic Macular Edema (DME) versus normal subjects. Addressing this classification problem has valuable interest since early detection and treatment of DME play a major role to prevent eye adverse effects such as blindness.

Despite previous works addressing this problem, this article points out the lack of publicly available data and benchmarking suited for this particular task of identify DME *vs. normal* SD-OCT volumes. The main contribution of this article is to cover these deficiencies by providing a common benchmark, dataset, and a collection of our own implementation of the most relevant methodologies found in the literature.

Index Terms—

I. INTRODUCTION

Eye diseases such as Diabetic Retinopathy (DR) and DME are the most common causes of irreversible vision loss in individuals with diabetes. Just in United States alone, health care and associated costs related to eye diseases are estimated at almost \$500 M [1]. Moreover, the prevalent cases of DR ares expected to grow exponentially affecting over 300 M people worldwide by 2025 [2]. Given this scenario, early detection and treatment of DR and DME play a major role to prevent adverse effects such as blindness. DME is characterized as an increase in retinal thickness within 1 disk diameter of the fovea center with or without hard exudates and sometimeso associated with cysts [3]. Fundus images which have proven to be very useful in revealing most of the eye pathologies [4, 5] are not as good as Optical Coherence Tomography (OCT) images which provide information about cross-sectional retinal morphology [6] (see Sect. III for some image examples). Therefore the growing interest in developing methodologies for OCT data. In this sense, great effort has been placed in retinal layers segmentation, which is a necessary step for retinal thickness measurements [7, 8].

However, few studies have addressed the specific problem of DME automatic detection in OCT, revealing large grounds to be covered in terms of: (i) manipulating OCT volumes, (ii) finding radiomix pathology signs, or (iii) appropriated classification strategies.

Advances in any of those regards is of great interest since (i) manual evaluation of SD-OCT volumetric scans is expensive and time consuming [9]. (ii) SD-OCT acquisition has some deficiencies due to eye movement during the scan [10], the reflectivity nature of the retina [?], the fact that OCT suffers from high levels of noise and the overall image quality is inconsistent [?]. (iii) Coexistence of multiple pathologies [10], easy to miss pathology signs [9], or large variability within the pathology treats which difficult to obtain proper radiomix to facilitate the task of classification.

The rest of this article is structured as follows: Section ?? offers a general idea of the literature state-of-the-art in SD-OCT volume classification. Section III reviews some publicly available datasets and states the need for another one that suits the classification task here described. Section IV proposes an experimental benchmark to compare different methodologies presented in Sect. ??. Section V reports and discusses the obtained results, while Sect. VII wraps up our thoughts regarding this work and its possible direction.

II. BACKGROUND

This section reviews works straightly addressing the problem of classifying OCT volumes as normal or abnormal, regardless of the target pathology. The methods are categorized in terms of its learning strategy, namely: supervised or semisupervised.

A. Supervised methods

Supervised classification is based on full annotated and labeled training set. In such methods the labeled training data is used to train the classifier function, which is latter used for prediction. Figure 2 describes a prevalent structure for supervised classification. The volumes undergo: (i) *Pre-processing* to reduce the natural noise of the images and correct acquisition deficiencies; (ii) *Feature detection* to quantify visual cues like appearance, texture, shape, etc. (iii) *Mapping* to determine the discrete set of elements (structures) to represent the sample to be classified (i.e.B-scan/volume); (iv) *Feature representation* to associate a descriptor for each

element from the *mapping-stage*. This descriptor packages the visual cues associated to the sample. (v) *Classification*.

Venhuizen et al. propose a classification method to distinguish between Age-related Macular Degeneration (AMD) and normal SD-OCT volumes using Bag-of-Words (BoW) models [9]. The method detects and selects a set of keypoints at each individual B-scan. Essentially, keeping the salient points comprised at the top 3% of the vertical gradient values. Then, a texton of size 9×9 pixels is extracted around each keypoint, and Principal Component Analysis (PCA) is applied to reduce the dimension of every texton to get a feature vector of size 9. All extracted feature vectors are used to create a codebook using k-means clustering. Then, each OCT volume is represented in terms of this codebook and is characterized as a histogram that captures the codebook occurrences. These histograms are used as feature vector to train a Random Forest (RF) with a maximum of 100 trees. The method is tested using a publicly available dataset of 384 OCT volumes [?], achieving an Area Under the Curve (AUC) of 0.984.

Srinivasan et al. [11] propose a classification method to distinguish DME, AMD and normal SD-OCT volumes. The OCT images are pre-processed by first enhancing sparsity in a transform-domain (BM3D [?]), to reduce their speckle noise, and then by flattening the retinal curvature to reduce the interpatient variations. Histogram of Oriented Gradients (HOG) features are then extracted from multi-resolution pyramid of each pre-processed slice of a volume. These features are classified using a linear Support Vector Machines (SVM). Note that the method classifies each individual B-scan into one of three categories, i.e.DME, AMD, and normal, and then classifies a volume based on the number of B-scans in each category. This method is also tested using a publicly available dataset, composed of 45 patients equally subdivided into the three target classes. The method achieves a correct classification rate of 100%, 100% and 86.67% for normal, DME and AMD patients, respectively.

Alsaih et al. [?] extended Srinivasan et al. [11] by (i) incorporating Local Binary Patterns (LBP) to the feature detection stage; and (ii) adding PCA to the feature representation step, as proposed by Venhuizen et al. [9];

Lemaitre et al. [12] propose a method based on LBP features to describe the texture of OCT images and dictionary learning using the BoW models [13]. Note that using BoW and dictionary learning contrary to [11] the classification is performed per volume, rather than B-scan. In this method the OCT images are first pre-processed using Non-Local Means (NLM) filtering, to reduce the speckle noise. Then the volumes are mapped into discrete set of structures namely: local, when these structures correspond to patches; or global, when they correspond to volume slices or the whole volume. According to different mapping, LBP or LBP from Three Orthogonal Planes (LBP-TOP) texture features are extracted and represented (per volume) using histogram, PCA or BoW. The final feature descriptors per volumes are classified using RF classifier. This methodology was tested against Venhuizen et al. [9] using public and non-public datasets showing an improvement within the results by achieving a Sensitivity (SE) of 87.5% and a Specificity (SP) of 75%.

Liu et al. propose a methodology aiming for B-scan classification, rather than volume classification. The classification goal is to distinguish between macular pathology and normal OCT B-scan images using LBP and gradient information as attributes [10]. The method starts by aligning and flattening the images and creating a 3-level multi-scale spatial pyramid. The edge and LBP histograms are then extracted from each block of every level of the pyramid. All the obtained histograms are concatenated into a global descriptor whose dimensions are reduced using PCA. Finally a SVM with an Radial Basis Function (RBF) kernel is used as classifier. The method achieved good results in detection of OCT scan containing different pathology such as DME or AMD, with an AUC of 0.93 using a dataset of 326 OCT scans.

Albarrak et al. [?] propose another volumetric classification framework for differentiating AMD and normal volumes. The author propose to flatten the volume of interest (VOI) from each OCT volume as a pre-processing step and extract LBP-TOP and HOG+LBP-TOP features from individual subvolumes within each VOI. The extracted features were concatenated into a single feature vector per OCT volume and presented in lower dimensions using PCA. Finally a Bayesian network classifier was used for classifying the volumes. Testing their proposed method and comparing with [10] using 140 OCT volumes, they achieved the highest SE and SP of 92.4% and 90.5%, respectively.

Anantrasirichai et al. [?] propose to detect glaucoma in OCT images based on a variety of texture measures. The images are described in terms of LBP, Gray-level co-occurrence matrix (GLCM), wavelet, granulometry, run length measures, and intensity level distributions in combination with retinal layer thickness without any pre-processing. Using PCA and linear and kernel-SVM classifier, the authors compared the performance of individual features and their combinations. Testing with rather a small dataset of 24 OCT voluems, their proposed method achieved an Accuracy (ACC) of 81.95% while using layer thickness information.

B. Semi-supervised methods

An example of semi-supervised approach for SD-OCT classification is recently proposed by Sankar. *et al.* [?]. The proposed method is based on appearance modeling of normal OCT images using Gaussian Mixture Model (GMM) and anomaly detection. The abnormal B-scans are detected as outliers to the fitted GMM and volume classification is performed based on the number of detected outliers in the volume.

10

20 This approach differs from supervised approaches since the B-scan detection method does not require a labeled training set of B-scans. This method starts by pre-processing the B-scans using resizing, flattening and denoising (NLM filter). The features are extracted by taking the intensity information of each B-scan and applying PCA to reduce their dimension. The feature space is then modeled using GMM. In the testing

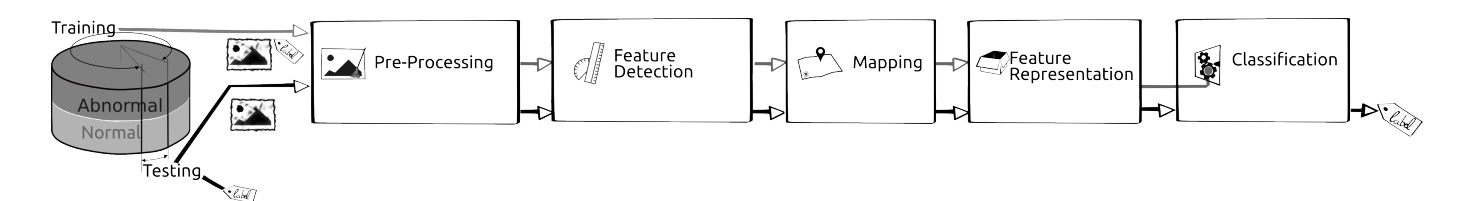


Fig. 1. Common framework

stage, for the new B-scan, the features are extracted in a similar way and they are classified as normal or abnormal based on their Mahalanobis distance to the GMM. Finally the volume classification is performed considering the umber of outliers (abnormal) B-scans per volume.

III. DATA

A common dataset is required to compare different methodologies. Despite the fact that lack of public data is a common claim in the medical image community [?], the ophtalmic community has recently made available public dataset, mainly gathered at Duke University [?, 11] and used by Venhuizen *et al.* [9] as well as Srinivasan *et al.* [11]. However, these dataset are not suitable for our problem.

Venhuizen *et al.* have evaluated their framework on a large public dataset of 384 OCT annotated volumes classified either as AMD or normal cases. Our goal, however, remains to focus on the detection of DME rather than AMD, despite the interest of testing the frameworks against a large dataset.

In the contrary, Srinivasan *et al.* have tested their framework using a public dataset containing AMD, DME, and normal volumes [11]. The data, however, have been denoised, aligned, and cropped, without access to the original set of images.

IV. EXPERIMENTAL SETUP

The experimental set-up is summarized in table I. Where the most relevant works in Sect. ?? are formulated as the as the 5-steps standard classification procedure described in Fig. 2.

A. Implementation details

For reproductivity purposes, the experimentation described in this work can be found in [?], where the image processing and Machine Learning (ML) rapid pipeline prototyping library *Protoclass* [?] has been used to implement the methodologies in Tab. I in accordance to proposed experimentation framework. Each methodology implementation can be seen as a

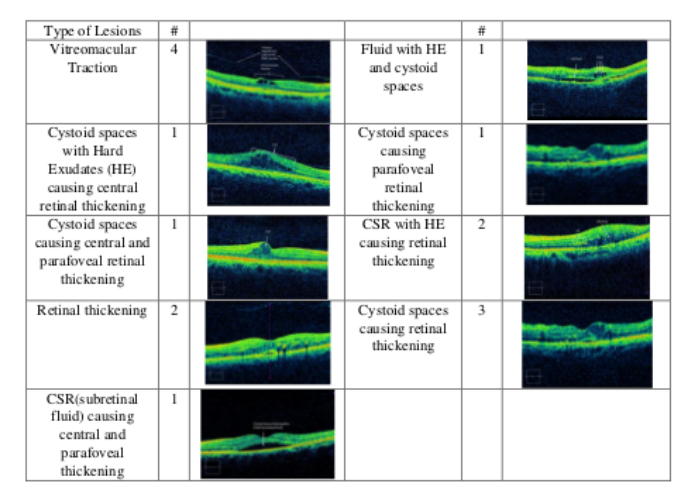


Figure 2. Example of the DME dataset

190

Fig. 2. SERI dataset description.

TABLE II

CORRESPONDENCE BETWEEN THE MOST RELEVANT METHODOLOGIES
REVIEWED IN SECT. ?? AND THE PROPOSED EXPERIMENTAL FRAMEWORK,

195	Ref	Pre-processing	Features	Mapping	Representation	Classification
Venl	nuizen et al. [9, ?]		Texton	Local	BoW, PCA	RF
Srin	ivasan et al. [11, ?]	De-noise Flatten Cropped	HOG	Global		linear-SVM
200 _{Lem}	aitre et al. [12, ?]	De-noised	LBP LBP-TOP	Local Global	PCA, BoW, Histogram	RF
Alsa	ih <i>et al</i> . [?]	*******	LBP LBP-TOP	*****	PCA, BoW, *******	RF
Sanl	car et al. [?, ?]	De-noised Flatten Cropped	Pixel -intensities	Global	PCA	Mahalanobis -distance to GMM

plug-in to experiment in [?], while references to stand-alone implementation of these methodologies can be found in Tab. I. All the repositories are publicly available and provided with tests to ensure that our implementation agrees with the results ²¹⁰/₂ ported by the original works. ¹

B. Evaluation

All the experiments are evaluated in terms of SE and SP (see Eq. 1) using the Leave-One-Patient Out Cross-Validation (LOPO-CV) strategy, in line with [12]. The SE evaluates the

¹Note that methodologies where this quality control could not had been enforced have been discarded for experimentation and only reviewed based on the results reported by the original work and compiled in Sect. ??.

TABLE I Summary of the classification performance in terms of SE and SP in (%).

	Srinivasan et al. [11]	Venhuizen et al. [9]	Alsaih et al. [?]	Lemaitre et al. [12]	Sankar et al. [?]
SE	68.8	61.5	75.0	87.5	93.8
SP	93.8	58.8	87.5	75.0	80.0

performance of the classifier with respect to the positive class, while the SP evaluates its performance with respect to negative class.

$$SE = \frac{TP}{TP + FN}$$
 $SP = \frac{TN}{TN + FP}$ (1)

The use of LOPO-CV implies that at each round, a pair DME-normal volume is selected for testing while the remaining volumes are used for training. Subsequently, no SE or SP variance can be reported. However, LOPO-CV strategy has been adopted despite this limitation due to the reduced size of the dataset.

V. RESULTS AND DISCUSSION

Table ?? shows the results obtained in terms of SE and SP, where Sankar *et. al.* achieve the best performance, revealing that DME lesions can be modeled accurately based only on a set of normal SD-OCT volumes.

VI. CONCLUSION AND FURTHER WORK

The work here presented states the relevance of developing methodologies to automatically differentiate DME *vs. normal* SD-OCT scans. This article offers an overview of the state-of-the-art methodologies and provides a public benchmarking to facilitate further studies. In this regard, there are two crucial aspects to improve the work here presented: (i) enlarge the dataset. (ii) reach out for the original authors of those methods in Sect. ?? that could not be included in Sect. IV because our implementation could not be tested against the original data or we did not achieve the original results.

REFERENCES

- S. Sharma, A. Oliver-Hernandez, W. Liu, and J. Walt, "The impact of diabetic retinopathy on health-related quality of life," *Current Opinion in Ophtalmology*, vol. 16, pp. 155–159, 2005.
- [2] S. Wild, G. Roglic, A. Green, R. Sicree, and H. King, "Global prevalence of diabetes estimates for the year 2000 and projections for 2030," *Diabetes Care*, vol. 27, no. 5, pp. 1047–1053, 2004.
- [3] Early Treatment Diabetic Retinopathy Study Group, "Photocoagulation for diabetic macular edema: early treatment diabetic retinopathy study report no 1," JAMA Ophthalmology, vol. 103, no. 12, pp. 1796–1806, 1985
- [4] M. R. K. Mookiah, U. R. Acharya, C. K. Chua, C. M. Lim, E. Ng, and A. Laude, "Computer-aided diagnosis of diabetic retinopathy: A review," *Computers in Biology and Medicine*, vol. 43, no. 12, pp. 2136–2155, 2013.
- [5] E. Trucco, A. Ruggeri, T. Karnowski, L. Giancardo, E. Chaum, J. Hubschman, B. al Diri, C. Cheung, D. Wong, M. Abramoff, G. Lim, D. Kumar, P. Burlina, N. M. Bressler, H. F. Jelinek, F. Meriaudeau, G. Quellec, T. MacGillivray, and B. Dhillon, "Validation retinal fundus image analysis algorithms: issues and proposal," *Investigative Ophthalmology & Visual Science*, vol. 54, no. 5, pp. 3546–3569, 2013.

- [6] Y. T. Wang, M. Tadarati, Y. Wolfson, S. B. Bressler, and N. M. Bressler, "Comparison of Prevalence of Diabetic Macular Edema Based on Monocular Fundus Photography vs Optical Coherence Tomography," *JAMA Ophthalmology*, pp. 1–7, Dec 2015.
- [7] S. J. Chiu, X. T. Li, P. Nicholas, C. A. Toth, J. A. Izatt, and S. Farsiu, "Automatic segmentation of seven retinal layers in sd-oct images congruent with expert manual segmentation," *Optic Express*, vol. 18, no. 18, pp. 19413–19428, 2010.
- [8] R. Kafieh, H. Rabbani, M. D. Abramoff, and M. Sonka, "Intra-retinal layer segmentation of 3d optical coherence tomography using coarse grained diffusion map," *Medical Image Analysis*, vol. 17, pp. 907–928, 2013.
- [9] F. G. Venhuizen, B. van Ginneken, B. Bloemen, M. J. P. P. van Grisven, R. Philipsen, C. Hoyng, T. Theelen, and C. I. Sanchez, "Automated agerelated macular degeneration classification in OCT using unsupervised feature learning," in SPIE Medical Imaging, vol. 9414, 2015, p. 941411.
- [10] Y.-Y. Liu, M. Chen, H. Ishikawa, G. Wollstein, J. S. Schuman, and R. J. M., "Automated macular pathology diagnosis in retinal oct images using multi-scale spatial pyramid and local binary patterns in texture and shape encoding," *Medical Image Analysis*, vol. 15, pp. 748–759, 2011.
- [11] P. P. Srinivasan, L. A. Kim, P. S. Mettu, S. W. Cousins, G. M. Comer, J. A. Izatt, and S. Farsiu, "Fully automated detection of diabetic macular edema and dry age-related macular degeneration from optical coherence tomography images," *Biomedical Optical Express*, vol. 5, no. 10, pp. 3568–3577, 2014.
- [12] G. Lemaitre, M. Rastgoo, J. Massich, S. Sankar, F. Meriaudeau, and D. Sidibe, "Classification of SD-OCT volumes with LBP: Application to dme detection," in *Medical Image Computing and Computer-*Assisted Intervention (MICCAI), Ophthalmic Medical Image Analysis Workshop (OMIA), 2015.
- [13] J. Sivic and A. Zisserman, "Video google: a text retrieva approach to object matching in videos," in *IEEE ICCV*, 2003, pp. 1470–1477.
- [14] G. Lemaitre, M. Rastgoo, and J. Massich, "retinopathy: Jo-omia-2015," Nov. 2015. [Online]. Available: http://dx.doi.org/10.5281/zenodo.34277

250